

Implications of the $Z_{cs}(3985)$ and $Z_{cs}(4000)$ as two different states

Lu Meng,¹ Guang-Juan Wang,^{2,*} Bo Wang,^{3,†} and Shi-Lin Zhu^{4,‡}

¹Ruhr-Universität Bochum, Fakultät für Physik und Astronomie,
Institut für Theoretische Physik II, D-44780 Bochum, Germany

²Advanced Science Research Center, Japan Atomic Energy Agency, Tokai, Ibaraki, 319-1195, Japan

³School of Physical Science and Technology, Hebei University, Baoding 071002, China

⁴School of Physics and Center of High Energy Physics, Peking University, Beijing 100871, China

In this work, we explore the implications of the narrower state $Z_{cs}(3985)$ in BESIII and the wider state $Z_{cs}(4000)$ in LHCb as two different states. We treat them as two $|\bar{D}_s D^*/\bar{D}_s^* D\rangle$ di-meson resonances with different hadronic components in a solvable nonrelativistic effective field theory. We include the possible violations of heavy quark spin symmetry and SU(3) flavor symmetry. Treating them as two states, our results show that $Z_{cs}(4000)$ is the pure $(|\bar{D}_s^* D\rangle + |\bar{D}_s D^*\rangle)/\sqrt{2}$ state, which is the partner of $Z_c(3900)$ in the SU(3) flavor symmetry limit. The $Z_{cs}(3985)$ is the $(|\bar{D}_s^* D\rangle - |\bar{D}_s D^*\rangle)/\sqrt{2}$ state. Our calculations also imply the existence of a tensor $\bar{D}_s^* D^*$ resonance as the heavy quark spin symmetry partner of the $Z_{cs}(3985)$ state. Its mass and decay width are 4126 MeV and 13 MeV, respectively. Meanwhile, the decay $Z_{cs}(3985) \rightarrow J/\psi K$ is suppressed by the heavy quark spin symmetry. Searching for the tensor $\bar{D}_s^* D^*$ state and the $Z_{cs}(3985) \rightarrow J/\psi K$ decay mode in experiments would be helpful to test the prerequisite that $Z_{cs}(3985)$ and $Z_{cs}(4000)$ are two different states.

I. INTRODUCTION

Recently, the LHCb and BESIII collaborations made great breakthroughs in searching for hidden charmed multi-quark states with strangeness [1–3] (for general reviews on the exotic hadrons, see Refs. [4–9]). LHCb collaboration obtained the first evidence of the pentaquark state with strangeness [1], which had been predicted as the partner of P_c states [10–12]. BESIII collaboration reported a structure $Z_{cs}(3985)^-$ in the K^+ recoil-mass spectra in the $e^+e^- \rightarrow K^+(D_s^- D^{*0} + D_s^{*-} D^0)$ with 5.3σ [2]. Several months later, LHCb collaboration announced the observation of two strange hidden charm states, $Z_{cs}(4000)^+$ and $Z_{cs}(4220)^+$ in the invariant mass spectrum of the $J/\psi K^+$ channel in the $B^+ \rightarrow J/\psi \phi K^+$ process with the significance of 15σ and 5.9σ , respectively [3]. Before these experimental observations, the hidden charm and bottom tetra- and pentaquarks with strangeness were also investigated in Ref. [13].

The observation of $Z_{cs}(3985)^-$ in BESIII inspired amounts of theoretical works to explore its nature [14–41], which had been released before the observation of $Z_{cs}(4000)$ and $Z_{cs}(4220)$ in LHCb collaboration. The most popular interpretation of the $Z_{cs}(3985)$ is the $\bar{D}_s D^*/\bar{D}_s^* D$ di-meson state, which is the SU(3) flavor [SU(3)_F] symmetry partner of the $Z_c(3900)$ [42, 43]. A natural prediction is a vector $\bar{D}_s^* D^*$ di-meson state as the heavy quark spin symmetry (HQSS) partner of the $Z_{cs}(3985)$ and the SU(3)_F partner of the $Z_c(4020)$ [44]. The typical features or assumptions of above interpretations are the good HQSS and SU(3)_F symmetry.

The $Z_{cs}(4000)$ was observed in LHCb in the proximity of the $\bar{D}_s D^*/\bar{D}_s^* D$ thresholds like the $Z_{cs}(3985)$. However, the width of $Z_{cs}(4000)$ is over 100 MeV, which is about ten times larger than that of $Z_{cs}(3985)$ as shown in Fig. 1 and

Table I. Moreover, the $Z_{cs}(4220)$ state with higher mass is also a much broader resonance than the theoretical predictions of the HQSS partner of $Z_{cs}(3985)$ [14–18]. Thus, theorists started to consider the $Z_{cs}(4000)$ and $Z_{cs}(3985)$ as two different states in the hadronic molecular scheme [45] and the compact tetraquark scheme [46]. The observations in LHCb also triggered a new round of theoretical investigations on the Z_{cs} states [47–50].

In our previous works [14, 18], we investigated the $Z_{cs}(3985)$ state in the HQSS and SU(3)_F symmetry limits. In order to illustrate the components of $Z_{cs}(3985)$, the concept of G parity was extended to the U -spin and V -spin sectors [14]. The G_I , G_U and G_V parities are defined as

$$\hat{G}_I = \hat{C}e^{i\hat{I}_2\pi}, \quad \hat{G}_U \equiv \hat{C}e^{i\hat{U}_2\pi}, \quad \hat{G}_V \equiv \hat{C}e^{i\hat{V}_2\pi}, \quad (1)$$

where G_I is the conventional G -parity and $G_{U/V}$ is the analog in U/V -spin sector. In the SU(3)_F symmetry limit, they are conserved. The di-meson wave functions of $Z_c(3900)$ or $Z_{cs}(3985)$ with $G_{I/U/V}$ -parity reads

$$|\bar{P}V/\bar{V}P, G_{I/U/V}\rangle = \frac{1}{\sqrt{2}} (|\bar{P}V\rangle + G_{I/U/V}|\bar{V}P\rangle), \quad (2)$$

where P and V are the pseudoscalar and vector heavy-light mesons, respectively. In this work, we use the quantum number I for the strangeless system, V for the $|s\bar{u}\rangle$ system and U for the $|s\bar{d}\rangle$ system. In Refs. [14] and [18], we assigned $Z_{cs}(3985)$ as the partner state of $Z_c(3900)$ due to their consistent masses with respect to thresholds, widths and line shapes. We also predicted the HQSS partner of $Z_{cs}(3985)$ and SU(3)_F partner of $Z_c(4020)$, a state with a mass around 4130 and width around 30 MeV. The main assumptions and predictions in Refs. [14] and [18] are presented in Fig. 2.

In this work, we will explore the possibility of $Z_{cs}(3985)$ and $Z_{cs}(4000)$ as two different di-meson resonances. We will introduce the violation effects of HQSS and SU(3)_F symmetry in the framework of a solvable nonrelativistic effective field theory (NREFT). Our numerical results and phenomenological analysis will provide several important consequences

* wj@pku.edu.cn

† bo-wang@pku.edu.cn

‡ zhul@pku.edu.cn

of $Z_{cs}(3985)$ and $Z_{cs}(4000)$ as two different states, including their hadronic components, selection rules of the decay and the existence of a tensor $\bar{D}_s^* D^*$ di-meson state. Due to the large uncertainties of the mass and width of $Z_{cs}(4220)$, we only consider its qualitative properties, a wide resonance above the $D_s^* \bar{D}^*$ threshold about 100 MeV.

The work is organized as follows. In Sec. II, we will analyze the symmetries and possible violations for the $Z_{cs}(3985)$ and $Z_{cs}(4000)$ states. In Sec. III, we construct a solvable NREFT to investigate the Z_c and Z_{cs} states as the di-meson resonances. In Sec. IV, we combine the numerical results from NREFT and the experimental results to provide several implications. Finally, we make a brief conclusion in Sec. V. In Appendix A, we give the details to solve the Lippmann-Schwinger equations (LSEs) with a separable potential.

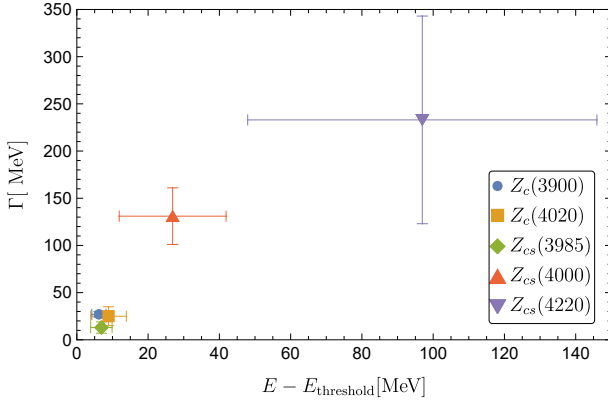


FIG. 1. Masses with respect to relevant thresholds and decay widths of Z_c and Z_{cs} states [2, 3, 51, 52]. The corresponding thresholds are listed in Table I.

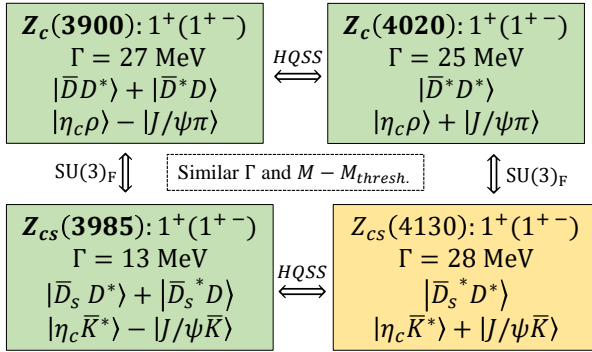


FIG. 2. The implications of $Z_{cs}(3985)$ as the $SU(3)_F$ symmetry partner of $Z_c(3900)$ [14, 18]. The green cards and the bold particle names are used to label the states observed in experiments. Our predictions are presented in the yellow cards. The quantum numbers $I^{G_I}/U^{G_U}/V^{G_V} (J^{PC})$ of the states are given in the first row of each card. Γ is the decay width. The hadronic components are listed in the third row of each card. In the last row, the wave function after rearrangement in the basis of $|(c\bar{c})(q_1\bar{q}_2)\rangle$ is given.

II. SYMMETRIES AND THEIR VIOLATIONS

The Hamiltonian of the $\bar{D}_{(s)}^{(*)} D_{(s)}^{(*)}$ di-meson systems can be divided into the free part \hat{H}_0 and the interacting part \hat{V} ,

$$\hat{H} = \hat{H}_0 + \hat{V}, \quad \hat{H}_0 = m_a + m_b + \frac{\hat{p}^2}{2\mu_{ab}}, \quad (3)$$

where $m_{a/b}$ and μ_{ab} are the mass of the a/b particle and their reduced mass, respectively. The $SU(3)_F$ symmetry and HQSS are both approximate symmetries of Eq. (3). For the near-threshold states, the interaction is weak. In Ref. [53], we have showed that the leading violations of the two symmetries arise from the mass terms in Eq. (3). There are two large mass splittings compared to the interaction \hat{V} ,

$$m_{D_s^{(*)}} - m_{D^{(*)}} \simeq 100 \text{ MeV}, \quad (4)$$

$$m_{D_{(s)}^*} - m_{D_{(s)}} \simeq 140 \text{ MeV}, \quad (5)$$

which will break the $SU(3)_F$ symmetry and HQSS, respectively. In addition, we also introduce the symmetry breaking effects in the interaction.

A. Heavy quark spin symmetry

In the spin space, the eigenvector of \hat{H}_0 reads,

$$\begin{cases} J^P = 0^+, & |\bar{P}P\rangle \\ J^P = 1^+, & \cos \alpha |\bar{P}V\rangle - \sin \alpha |\bar{V}P\rangle \\ J^P = 1^+, & \sin \alpha |\bar{P}V\rangle + \cos \alpha |\bar{V}P\rangle \\ J^P = 0^+/1^+/2^+, & |\bar{V}V\rangle, \end{cases} \quad (6)$$

The mixing effect among $|\bar{P}P\rangle$, $|\bar{P}V/\bar{V}P\rangle$, and $|\bar{V}V\rangle$ states with the same quantum number would be suppressed by the mass splittings in Eq. (5). The $|\bar{P}V\rangle$ and $|\bar{V}P\rangle$ states are (almost) degenerate for the free Hamiltonian and will mix with each other (The thresholds of $D_s^- D^{*0}$ and $D_s^{*-} D^0$ are 3975 MeV and 3977 MeV, respectively). The mixing angle will be determined by the interaction \hat{V} .

The interaction in the spin space could be introduced as [54, 55],

$$V^s = V_{q\bar{q}}^s + \text{HQSS breaking terms}, \quad (7)$$

$$V_{q\bar{q}}^s = c_1^s + c_2^s \mathbf{s}_q \cdot \mathbf{s}_{\bar{q}}, \quad (8)$$

where $V_{q\bar{q}}^s$ is the interaction between the light degrees of freedom, which satisfies the HQSS. The $\mathbf{s}_{q/\bar{q}}$ is the spin operator of the light (anti)-quark. c_1^s and c_2^s are two independent coupling constants.

For the $|\bar{P}V/\bar{V}P\rangle$ states, the hadronic interactions in the $\{|\bar{P}V, \bar{V}P\rangle\}$ basis read,

$$\langle V^s \rangle_{\{\bar{P}V, \bar{V}P\}}^{1^+} = \begin{bmatrix} c_1^s & -\frac{1}{4}c_2^s \\ -\frac{1}{4}c_2^s & c_1^s + \delta c^s \end{bmatrix}, \quad (9)$$

In the HQSS, the interactions in the $|\bar{P}V/\bar{V}P\rangle$ channels are the same. We introduce the δc^s in the diagonal term to account

TABLE I. Masses, widths and relevant two-meson thresholds for the Z_c and Z_{cs} states (in units of MeV). The statistical and systematical errors have been added in quadrature.

	$Z_c(3900)^+$ [51]	$Z_c(4020)^+$ [44]	$Z_{cs}(3985)^-$ [2]	$Z_{cs}(4000)^+$ [3]	$Z_{cs}(4220)^+$ [3]
M	3882 ± 2	4026 ± 5	3983 ± 3	4003 ± 15	4216 ± 49
Γ	27 ± 3	25 ± 10	13 ± 6	131 ± 30	233 ± 110
Threshold	$\bar{D}^0 D^{*+} / \bar{D}^{*0} D^+$	$\bar{D}^{*0} D^{*+}$	$D_s^- D^{*0} / D_s^{*-} D^0$	$\bar{D}^{*0} D_s^+ / \bar{D}^0 D_s^{*+}$	$\bar{D}^{*0} D_s^{*+}$
	3876	4017	3976	3976	4119

for the HQSS violation effect. In the HQSS limit ($\delta c^s = 0$), the mixing angle in Eq. (6) could be determined,

$$|\bar{P}V/\bar{V}P, +\rangle = \frac{1}{\sqrt{2}} (|\bar{P}V\rangle + |\bar{V}P\rangle), \quad (10)$$

$$|\bar{P}V/\bar{V}P, -\rangle = \frac{1}{\sqrt{2}} (|\bar{P}V\rangle - |\bar{V}P\rangle), \quad (11)$$

where the relative signs of two hadronic components are used to label the states. For the $[\bar{D}D^*/\bar{D}^*D]^{I=1}$ and $\bar{D}_s D^*/\bar{D}_s^* D$ states, the sign is that of the $G_{I/U/V}$ -parity as shown in Eq. (2) (see Ref. [14] for details). In this basis, the interaction in Eq. (9) reads,

$$\langle V^s \rangle_{\{\bar{P}V/\bar{V}P, \pm\}}^{1+} = \begin{bmatrix} c_1^s - \frac{c_2^s}{4} + \frac{\delta c^s}{2} & -\frac{\delta c^s}{2} \\ -\frac{\delta c^s}{2} & c_1^s + \frac{c_2^s}{4} + \frac{\delta c^s}{2} \end{bmatrix} \quad (12)$$

which will become diagonal in the HQSS limit. Another two related channels are the $|\bar{V}V, 1^+\rangle$ and $|\bar{V}V, 2^+\rangle$. Their interactions in the HQSS limit read,

$$\langle V_{q\bar{q}}^s \rangle_{\{\bar{V}V\}}^{1+} = \langle V_{q\bar{q}}^s \rangle_{\{\bar{P}V/\bar{V}P, +\}}^{1+} = c_1^s - \frac{1}{4}c_2^s, \quad (13)$$

$$\langle V_{q\bar{q}}^s \rangle_{\{\bar{V}V\}}^{2+} = \langle V_{q\bar{q}}^s \rangle_{\{\bar{P}V/\bar{V}P, -\}}^{1+} = c_1^s + \frac{1}{4}c_2^s. \quad (14)$$

The two equalities indicate the existence of HQSS partners. For example, $Z_c(3900)$ and $Z_c(4020)$ have the similar masses with respect to the corresponding thresholds and decay widths, which stems from the Eq. (13). We are going to see the existence of other HQSS partners in the Z_{cs} sector.

We can rewrite the above four states on the basis of the heavy quark symmetry $|S_{\bar{c}c}^P, S_{q_1\bar{q}_2}^P; J^P\rangle$,

$$|\bar{P}V/\bar{V}P, +\rangle = \frac{1}{\sqrt{2}} (|0_{\bar{c}c}^-, 1_{q_1\bar{q}_2}^-, 1^+\rangle - |1_{\bar{c}c}^-, 0_{q_1\bar{q}_2}^-, 1^+\rangle), \quad (15)$$

$$|\bar{P}V/\bar{V}P, -\rangle = |1_{\bar{c}c}^-, 1_{q_1\bar{q}_2}^-, 1^+\rangle, \quad (16)$$

$$|\bar{V}V, 1^+\rangle = \frac{1}{\sqrt{2}} (|0_{\bar{c}c}^-, 1_{q_1\bar{q}_2}^-, 1^+\rangle + |1_{\bar{c}c}^-, 0_{q_1\bar{q}_2}^-, 1^+\rangle), \quad (17)$$

$$|\bar{V}V, 2^+\rangle = |1_{\bar{c}c}^-, 1_{q_1\bar{q}_2}^-, 2^+\rangle. \quad (18)$$

The wave function decomposition would give rise to a series of selection rules for the decay modes of the $\bar{D}^{(*)}D^{(*)}$ di-meson systems.

In the molecular model, the $Z_c(3900)$ and $Z_c(4020)$ are interpreted as the $|\bar{P}V/\bar{V}P, +\rangle$ and $|\bar{V}V, 1^+\rangle$, respectively (Apart

from the G -parity, the relative sign of the hadronic components of $Z_c(3900)$ could be also determined by the C -parity of the neutral one [14].). The interactions are the same except the HQSS breaking term as shown in Eq. (13). The existence of $Z_c(3900)$ and $Z_c(4020)$ as the partner states indicates that the HQSS is a good approximation. It is reasonable to infer a similar property for the $\bar{D}_s^{(*)}D^{(*)}$ systems. In this work, we will prove this conclusion by evaluating the HQSS breaking effect quantitatively. We also find that the $Z_{cs}(3985)$ and $Z_{cs}(4000)$ as two different states will imply the existence of a tensor $\bar{D}_s^* D^*$ state within HQSS.

B. $SU(3)_F$ symmetry

In this subsection, we adopt the light quark components to label the flavor of the di-meson systems. The leading $SU(3)_F$ breaking effect stems from the mass splitting in Eq. (4), which will suppress the mixing effect between $(|u\bar{u}\rangle + |d\bar{d}\rangle)/\sqrt{2}$ and $|s\bar{s}\rangle$ systems [53]. For the isovector and open strange systems, the $SU(3)_F$ violation effect starts to appear at the interaction terms. We introduce the interaction in the flavor space as follows,

$$V^f = c_1^f F_a^0 F_b^0 + c_2^f \sum_{i=1}^3 F_a^i F_b^i + c_3^f \sum_{i=4}^7 F_a^i F_b^i + c_4^f F_a^8 F_b^8, \quad (19)$$

with

$$F^i = \begin{cases} \frac{\lambda^i}{2} & \text{for quark} \\ -\frac{\lambda^{i*}}{2} & \text{for anti-quark} \end{cases}, \quad (20)$$

where λ^i is the Gell-mann matrix in the flavor space. $\lambda^0 = \sqrt{2/3}I$. In the $SU(3)_F$ limit, $c_2^f = c_3^f = c_4^f$. For the isovector and open strange systems, the elements of the interaction matrix read

$$\langle V^f \rangle_{\{d\bar{u}\}} = \frac{1}{12} (-2c_1 + 3c_2 - c_4), \quad (21)$$

$$\langle V^f \rangle_{\{s\bar{u}\}} = \frac{1}{6} (c_4 - c_1). \quad (22)$$

The difference between c_2^f and c_4^f leads to the $SU(3)_F$ violation effect for the two specific systems.

Unlike Ref. [14], we neither presume the $SU(3)_F$ symmetry is a good approximation nor relate the interaction of $[\bar{D}^{(*)}D^{(*)}]^{I=1}$ to those of $\bar{D}_s^{(*)}D^{(*)}$. We will show that the $Z_{cs}(3985)$ and $Z_{cs}(4000)$ as two different states imply the large $SU(3)_F$ violation effect.

III. SOLVABLE NREFT FOR RESONANCES

We adopt a solvable NREFT to investigate the Z_c and Z_{cs} states as the S -wave di-meson resonances. We construct the general contact S -wave interaction to the next-to-leading order,

$$V(\mathbf{p}, \mathbf{p}') = \frac{c_a}{\Lambda} + \frac{c_b}{\Lambda^3}(\mathbf{p}^2 + \mathbf{p}'^2), \quad (23)$$

where c_a and c_b are the low energy constants (LECs) for the leading order (LO) and the next-to-leading order (NLO). Λ is the cutoff scale. The possible $\mathbf{p} \cdot \mathbf{p}'$ term becomes vanishing after the partial wave expansion for the S -wave channel. Similar interaction was adopted in Refs. [14, 56]. We will take the symmetries and possible violation effects in Sec. II into consideration.

A. Single-channel formalism

In our calculation, we first adopt the single-channel formalism. The calculation in Ref. [14] has showed that the $Z_c(Z_{cs})$ couples to the $J/\psi\pi(K)$ channels weakly. Therefore, we only include the open-charmed $\bar{D}_{(s)}^{(*)}D^{(*)}$ channels. We deal with $\bar{P}V/\bar{V}P$ and $\bar{V}V$ channels separately, since their coupled-channel effect is suppressed by the mass splitting in Eq. (5). For the $Z_c(3900)$, $Z_c(4020)$, $Z_{cs}(3985)$ and $Z_{cs}(4000)$ states, we adopt four sets of independent LECs in Eq. (23), which will be determined by the mass and width of the corresponding state.

For the single-channel formalism, the Lippmann-Schwinger equation (LSE) reads,

$$T(\mathbf{p}, \mathbf{p}') = V(\mathbf{p}, \mathbf{p}') + \int \frac{d^3\mathbf{q}}{(2\pi)^3} \frac{V(\mathbf{p}, \mathbf{q})T(\mathbf{q}, \mathbf{p}')}{E - \frac{q^2}{2\mu} + i\epsilon}, \quad (24)$$

where E is the energy with respect to the threshold and μ is the reduced mass. We adopt the cutoff regularization (Λ is the cutoff parameter). A general numerical approach to solving the LSEs is the matrix-inversion method [57]. For this specific separable interaction, the LSEs can be solved analytically. In Appendix A, we adopt the technique in Ref. [58] and give the details to solve both the single-channel and coupled-channel LSEs. For the single-channel LSE, the on-shell solution reads,

$$\frac{1}{T(k)} = \frac{-G_0\Lambda^5 c_a - 2G_2\Lambda^3 c_b + (G_2^2 - G_0G_4)c_b^2 + \Lambda^6}{\Lambda^5 c_a + c_b [c_b (G_0k^4 - 2G_2k^2 + G_4) + 2k^2\Lambda^3]}, \quad (25)$$

where $k \equiv \sqrt{2\mu E}$ and $G_n(k)$ is defined as

$$G_n = \int \frac{d^3\mathbf{q}}{(2\pi)^3} \frac{q^n}{E - \frac{q^2}{2\mu} + i\epsilon}. \quad (26)$$

In the cutoff regularization scheme, we obtain the analytical expressions of G_n ,

$$G_0 = \frac{4\pi}{(2\pi)^3} 2\mu \left[k \tanh^{-1} \left(\frac{k}{\Lambda} \right) - \Lambda - i\frac{\pi}{2}k \right], \quad (27)$$

$$G_n = k^2 G_{n-2} - \frac{\mu}{\pi^2} \frac{\Lambda^{n+1}}{n+1}. \quad (28)$$

In order to describe the resonance, we make the analytical continuation to the nonphysical Riemann sheet. The resonance solution appears as the pole of the T -matrix in the nonphysical Riemann sheet. We fit the masses and decay widths in Table I and determine the LECs for the corresponding channels. We obtain the scattering lengths and effective ranges with the effective range expansion,

$$T^{-1}(k) = -\frac{\mu}{2\pi} \left(-\frac{1}{a_s} - ik + \frac{1}{2}r_0k^2 + \dots \right). \quad (29)$$

We fix the cutoff scale $\Lambda = 1.0$ GeV. Varying the cutoff parameter in a reasonable range will not change our results qualitatively. In Fig. II, we compare our results with those in Ref. [59]. In Ref. [59], the authors parameterized the T -matrix with the effective range expansion with truncation at the $\mathcal{O}(k^2)$.

B. Coupled-channel formalism

The $Z_{cs}(3985)$ and $Z_{cs}(4000)$ are the candidates of $|\bar{P}V/\bar{V}P, +\rangle$ and $|\bar{P}V/\bar{V}P, -\rangle$. We do not assign the specific corresponding relation for now. In general, the $|\bar{P}V/\bar{V}P, +\rangle$ and $|\bar{P}V/\bar{V}P, -\rangle$ states will couple with each other. The mixing effect arises from the HQSS breaking effect. In this subsection, we will adopt the coupled-channel formalism to evaluate the mixing effect numerically.

The coupled-channel potential for $Z_{cs}(3985)$ and $Z_{cs}(4000)$ systems can be parameterized as,

$$V(\mathbf{p}, \mathbf{p}')_{\{\bar{P}V/\bar{V}P, \pm\}} = \begin{bmatrix} \frac{c_a^+ + \delta c_a}{\Lambda} & \frac{\delta c_a}{\Lambda} \\ \frac{\delta c_a}{\Lambda} & \frac{c_a^- + \delta c_a}{\Lambda} \end{bmatrix} + \begin{bmatrix} \frac{c_b^+(\mathbf{p}^2 + \mathbf{p}'^2)}{\Lambda^3} & \\ & \frac{c_b^-(\mathbf{p}^2 + \mathbf{p}'^2)}{\Lambda^3} \end{bmatrix}, \quad (30)$$

where $c_{a/b}^{+/-}$ and δc_a are the LECs. The subscripts a and b represent the LO and NLO, respectively. The superscript $+/-$ labels the two channels. For the off-diagonal term, we only keep the LO interaction. For the coupled-channel systems with four available inputs (masses and widths of two resonances), we have five unknown LECs to be determined. Thus, a rigorous fitting to determine the mixing effect is not feasible.

The second best approach is to presume the mixing effect is negligible and then make a self-consistent test. We fix the c_a^+ , c_b^+ , c_a^- and c_b^- from the single-channel calculation and then vary δc_a to check whether the coupled-channel effect is ignorable or not. The δc_a is actually the HQSS breaking term and its meaning becomes clear when we change the coupled-channel potential into the $\{\bar{P}V, \bar{V}P\}$ basis,

$$V_{\{\bar{P}V, \bar{V}P\}}^{1+} = \frac{1}{2\Lambda} \begin{bmatrix} c_a^+ + c_a^- & c_a^+ - c_a^- \\ c_a^+ - c_a^- & c_a^+ + c_a^- + 4\delta c_a \end{bmatrix} + \text{NLO term}. \quad (31)$$

TABLE II. The scattering lengths a_s and effective ranges r_0 extracting from Z_c and Z_{cs} states within the single-channel NREFT (in units of fm). The results in Ref. [59] are listed for comparison. For the $Z_{cs}(3985)$ states, the two sets of results given in Ref. [59] correspond to two different choices of the thresholds.

		$Z_c(3900)$	$Z_c(4020)$	$Z_{cs}(3985)$	$Z_{cs}(4000)$
This work	a_s	-0.96 ± 0.09	-0.74 ± 0.24	-0.76 ± 0.26	-0.32 ± 0.07
	r_0	-2.88 ± 0.37	-3.95 ± 2.70	-6.70 ± 5.54	-2.08 ± 0.80
[59]	a_s	-0.85 ± 0.13	-1.04 ± 0.30	$-1.00 \pm 0.74(-1.28 \pm 0.60)$	-
	r_0	-2.52 ± 0.25	-3.90 ± 1.35	$-4.04 \pm 1.82(-3.65 \pm 1.60)$	-

We also define a ratio R_{HQSSB} as a reflection of the HQSS breaking effect

$$R_{\text{HQSSB}} = \frac{4\delta c_a}{|c_a^+ + c_a^-|}. \quad (32)$$

The nonzero R_{HQSSB} indicates the nonvanishing off-diagonal terms in Eq. (30). Then, the bases $|\bar{P}V/\bar{V}P, +\rangle$ and $|\bar{P}V/\bar{V}P, -\rangle$ will mix with each other. We define a mixing angle θ such that the states

$$\begin{cases} \cos\theta |\bar{P}V/\bar{V}P, +\rangle - \sin\theta |\bar{P}V/\bar{V}P, -\rangle \\ \sin\theta |\bar{P}V/\bar{V}P, +\rangle + \cos\theta |\bar{P}V/\bar{V}P, -\rangle \end{cases}, \quad (33)$$

could diagonalize the LO potential matrix. The θ reflects the significance of the coupled-channel effect.

We display the dependence of the mixing angle θ on the R_{HQSSB} in Fig. 3. In the HQSS limit, the $\theta = 0$. When we vary the R_{HQSSB} from -0.4 to 0.4 , the mix angle changes quite slightly, less than three degree and thus negligible. We also present the pole trajectories with varying R_{HQSSB} in Fig. 4. We find that the 40% HQSS breaking effect does not change the qualitative properties of two resonances. Their relative orders for the masses and widths do not change with the introduction of the HQSS breaking effect.

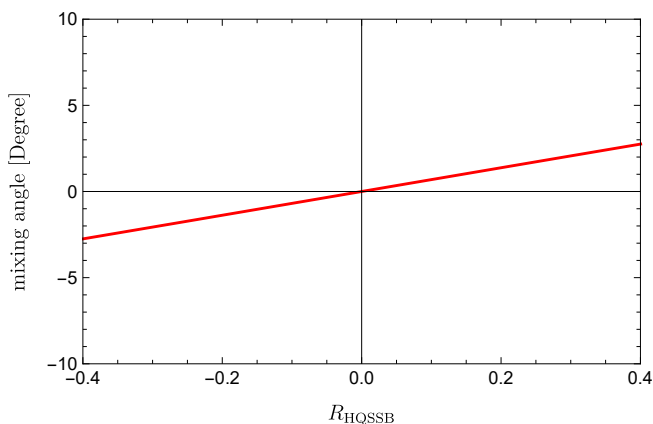


FIG. 3. The mixing angle of $|\bar{P}V/\bar{V}P, +\rangle$ and $|\bar{P}V/\bar{V}P, -\rangle$ for the Z_{cs} states with varying R_{HQSSB} .

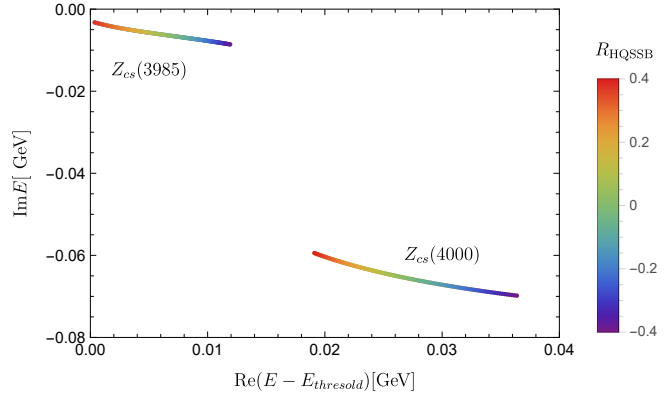


FIG. 4. The pole trajectories of the $Z_{cs}(3985)$ and $Z_{cs}(4000)$ states with varying R_{HQSSB} .

IV. PHENOMENOLOGICAL ANALYSIS

In this section, we combine the experimental results [2, 3, 60] and our calculations in Sec. III to analyze the implications of $Z_{cs}(3985)$ and $Z_{cs}(4000)$ as two different states. The main conclusions are illustrated in Fig. 5 and explained as follows,

1. *HQSS is a good approximation for the $\bar{D}_s^{(*)}D^{(*)}$ systems.* The consistent properties of $Z_c(3900)$ and $Z_c(4020)$ indicate that HQSS works well for $\bar{D}^{(*)}D^{(*)}$ systems. Meanwhile, the HQSS violation effect for the $|\bar{D}_s D^*/\bar{D}_s^* D, +\rangle$ and $|\bar{D}_s D^*/\bar{D}_s^* D, -\rangle$ systems is negligible. The 40% HQSS breaking effect will neither change the qualitative properties of two resonances as shown in Fig. 4, nor give rise to considerable mixing effect as shown in Fig. 3.
2. *$Z_{cs}(4000)$ and $Z_{cs}(4220)$ are the HQSS partners.* $Z_{cs}(4220)$ is a wide resonance above the $\bar{D}_s^* D^*$ threshold, though there are large uncertainties for its mass and width. It is natural to interpret it as $\bar{D}_s^* D^*$ resonances with $J^P = 1^+$. From Eq. (13), one finds that the interaction in the $Z_{cs}(4220)$ state is the same as that in the $|\bar{D}_s^* D/\bar{D}_s D^*, +\rangle$ state, which indicates its existence in the heavy quark limit. As a di-meson resonance, the decay of the Z_c or Z_{cs} state is dominated by decomposing into its ingredients. The $|\bar{D}_s^* D/\bar{D}_s D^*, +\rangle$ state should be a wide resonance as its HQSS partner $Z_{cs}(4220)$

because of the same interactions in the heavy quark limit. Thus, it is reasonable to infer that the wider resonance $Z_{cs}(4000)$ rather than the narrower resonance $Z_{cs}(3985)$ is the partner of the $Z_{cs}(4220)$ state.

3. $Z_{cs}(4000)$ and $Z_{cs}(3985)$ are almost pure $|\bar{D}_s^*D/\bar{D}_sD^*, +\rangle$ and $|\bar{D}_s^*D/\bar{D}_sD^*, -\rangle$ states, respectively. As the HQSS partner of $Z_{cs}(4220)$, the hadronic component of the $Z_{cs}(4000)$ is $|\bar{D}_s^*D/\bar{D}_sD^*, +\rangle$. If the $Z_{cs}(3985)$ is the second state near the $\bar{D}_s^*D/\bar{D}_sD^*$ threshold, it should be dominated by the $|\bar{D}_s^*D/\bar{D}_sD^*, -\rangle$ component. As shown in Fig. 3, the mixing effect of two different components is very tiny.
4. There should exist a tensor $\bar{D}_s^*D^*$ state as the HQSS partner of $Z_{cs}(3985)$. As illustrated in Eq. (14), the interaction in the tensor state $\langle V_{q\bar{q}}^s \rangle_{\{V\bar{V}\}}^{2+}$ is the same as that of $Z_{cs}(3985)$. With the interaction extracted from the $Z_{cs}(3985)$, we give a prediction of the mass and decay width of the tensor state,

$$M = 4126 \pm 3 \text{ MeV}, \quad \Gamma = 13 \pm 6 \text{ MeV}. \quad (34)$$
5. The branch ration $\mathcal{R}(Z_{cs} \rightarrow \bar{D}_s^*D/Z_{cs} \rightarrow \bar{D}_sD^*) \approx 0.5$ for $Z_{cs}(3985)$ or $Z_{cs}(4000)$ states. This is the consequence of that $Z_{cs}(4000)$ and $Z_{cs}(3985)$ are almost pure $|\bar{D}_s^*D/\bar{D}_sD^*, +\rangle$ and $|\bar{D}_s^*D/\bar{D}_sD^*, -\rangle$ states, respectively.
6. The decay mode $Z_{cs}(3985) \rightarrow J/\psi K$ is suppressed in the HQSS limit. In Eqs. (15)-(18), we decompose the $Z_{cs}(3985)$, $Z_{cs}(4000)$, $Z_{cs}(4220)$ and our prediction $Z_{cs}(4126)$ into the light and heavy degrees of freedom, which are separately conserved in the heavy quark limit. This leads to the a series of selection rules [61, 62] as displayed in Fig. 5. For instance, the decay process $Z_{cs}(3985) \rightarrow J/\psi K$ is forbidden within the HQSS due to the flip of the light degrees of freedom in the initial and final states. Another way to derive these selection rules is the conservation of the $G_{I/U/V}$ parity. For example, the $G_{U/V}$ parities of $Z_{cs}(3985)$, J/ψ and K are -1 , -1 and -1 , respectively. The decay $Z_{cs}(3985) \rightarrow J/\psi K$ is suppressed since the $G_{U/V}$ parity conservation is violated. The $G_{I/U/V}$ -parity encodes the information under the charge conjugation transformation, which is associated with the spin wave function. Thus, it is natural to obtain the same results from the HQSS decomposition and $G_{I/U/V}$ analysis. As illustrated in Fig. 5, the $Z_{cs}(3985)$ state is more likely to be observed in the $\bar{D}_s^*D/\bar{D}_sD^*$ channel, while it is hard to be observed in the $J/\psi K$ channel, which is consistent with the experimental results [2]. Similar results have also been obtained in Ref. [45]. Finally, one should note that the above selection rules of the $G_{I/U/V}$ parity may be violated by the $SU(3)_F$ flavor symmetry and heavy quark symmetry breaking effects.
7. The violation effect of the $SU(3)_F$ symmetry might be significant. As shown in Fig. 5, the widths of

the $Z_c(3900)$ and $Z_c(4020)$ states are much smaller than those of their $SU(3)_F$ partners $Z_{cs}(4000)$ and $Z_{cs}(4220)$. Moreover, the $I^{GJ}(J^{PC}) = 1^-(1^{++})$ state, the partner state of the $Z_{cs}(3985)$ in the $SU(3)_F$ limit, is missing in experiments. Therefore, the assignment of the $Z_{cs}(3985)$ and $Z_{cs}(4000)$ as two different states in Fig. 5 implies the large $SU(3)_F$ breaking effect.

The implications of $Z_{cs}(3985)$ and $Z_{cs}(4000)$ in Fig. 5 are quite different from the consequences of there existing only one $[\bar{D}_sD^*/\bar{D}_s^*D]^{1+}$ state in Fig. 2. In the theoretical aspects, the $Z_{cs}(3985)$ and $Z_{cs}(4000)$ as two different states imply that the $Z_{cs}(3985)$ is the $|\bar{D}_s^*D/\bar{D}_sD^*, -\rangle$ state, which is different from the assignment as the $|\bar{D}_s^*D/\bar{D}_sD^*, +\rangle$ in Fig. 2. This may lead to the different decay patterns in the $J/\psi K$ channel. With $Z_{cs}(3985)$ and $Z_{cs}(4000)$ as two different states, the decay $Z_{cs}(3985) \rightarrow J/\psi K$ is forbidden in the heavy quark limit, while the decay $Z_{cs}(3985) \rightarrow J/\psi K^*$ is not suppressed. Another additional tensor state $\bar{D}_s^*D^*$ is predicted as the HQSS partner of the $Z_{cs}(4000)$ in the two-state framework. If one assumes that there only exists one $[\bar{D}_sD^*/\bar{D}_s^*D]^{1+}$ state as shown in Fig. 2, no tensor partner is predicted and the $Z_{cs}(3985) \rightarrow J/\psi K$ decay mode is allowed in the HQSS limit. Meanwhile, the significant $SU(3)_F$ violation implied by $Z_{cs}(3985)$ and $Z_{cs}(4000)$ as two states contradicts the presuming $SU(3)_F$ symmetry in Fig. 2. In the experimental aspects, searching for the tensor $\bar{D}_s^*D^*$ state and the $Z_{cs}(3985) \rightarrow J/\psi K$ decay mode could help to check and clarify which assignment in Fig. 5 and Fig. 2 is reasonable.

V. CONCLUSION

In this work, we explore the implications of the narrower state $Z_{cs}(3985)$ observed in BESIII and the wider state $Z_{cs}(4000)$ in LHCb as two different states. We treat them as two $|\bar{D}_sD^*/\bar{D}_s^*D\rangle$ di-meson resonances with different hadronic components in a solvable NREFT. We consider the possible violation effect of the HQSS effect and that of the $SU(3)_F$ symmetry relating the Z_c states to Z_{cs} states. With the prerequisite of $Z_{cs}(3985)$ and $Z_{cs}(4000)$ as two different states, we obtain seven interesting consequences in theoretical and experimental aspects.

The theoretical consequences include the hadronic components of $Z_{cs}(4000)$ and $Z_{cs}(3985)$ as pure $|\bar{D}_s^*D/\bar{D}_sD^*, +\rangle$ and $|\bar{D}_s^*D/\bar{D}_sD^*, -\rangle$, respectively; The HQSS is a good approximation in the Z_c and Z_{cs} systems; The $Z_{cs}(4000)$ and $Z_{cs}(4220)$ are HQSS partners and the $SU(3)_F$ symmetry is violated significantly. Moreover, $Z_{cs}(4000)$ and $Z_{cs}(3985)$ as two different states provide three consequences that could be tested in the future experiments. The first one is the existence of a tensor $\bar{D}_s^*D^*$ resonance as the HQSS partner of $Z_{cs}(3985)$. Its mass and decay width are 4126 MeV and 13 MeV, respectively. The second one is the branch ratio $\mathcal{R}(Z_{cs} \rightarrow \bar{D}_s^*D/Z_{cs} \rightarrow \bar{D}_sD^*) \approx 0.5$ for $Z_{cs}(3985)$ and $Z_{cs}(4000)$ states, respectively. At last, the decay $Z_{cs}(3985) \rightarrow J/\psi K$ suffers from the suppression within the HQSS. Among them, the first and third experimental im-

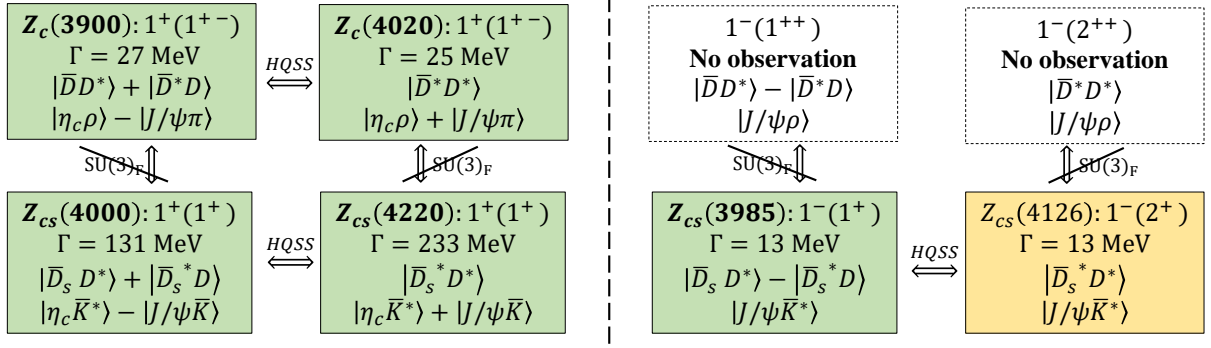


FIG. 5. Implications of $Z_{cs}(3985)$ and $Z_{cs}(4000)$ as two different states. The particles in green and yellow cards are observations and our predictions, respectively. For completeness, we list the information of two partner channels in white cards, which are neither the experimental resonances nor our theoretical predictions. The quantum numbers given in the first row of every cards is the $I^{G_I}/U^{G_U}/V^{G_V}(J^{PC})$ parity. The other notations are the same as those in Fig. 2.

plications could be used to distinguish the interpretation of the $Z_{cs}(3985)$ and $Z_{cs}(4000)$ as two different states from there only existing one $\bar{D}_s^* D/\bar{D}_s D^*$ resonance.

Appendix A: Solving LSEs with separable potentials

We use an example to illustrate the routine to solve the LSEs with the separable potentials. For the single-channel problem, the potential reads

$$V(\mathbf{p}', \mathbf{p}) = v^{aa} g(\mathbf{p}') g(\mathbf{p}) + v^{bb} f(\mathbf{p}') f(\mathbf{p}) + v^{ab} [f(\mathbf{p}') g(\mathbf{p}) + g(\mathbf{p}') f(\mathbf{p})], \quad (\text{A1})$$

where g and f are the functions of the momentum. $v^{aa/ab/bb}$ is the coefficient of the functions. The potential and the corresponding T -matrix can be factorized as

$$V(\mathbf{p}', \mathbf{p}) = \mathbb{L}(\mathbf{p}') \mathbb{V} \mathbb{R}(\mathbf{p}), \quad (\text{A2})$$

$$T(\mathbf{p}', \mathbf{p}) = \mathbb{L}(\mathbf{p}') \mathbb{T} \mathbb{R}(\mathbf{p}), \quad (\text{A3})$$

where

$$\mathbb{L}(\mathbf{p}) = [g(\mathbf{p}), f(\mathbf{p})], \quad \mathbb{R}(\mathbf{p}) = \begin{bmatrix} g(\mathbf{p}) \\ f(\mathbf{p}) \end{bmatrix}, \quad (\text{A4})$$

$$\mathbb{V}(E) = \begin{bmatrix} v^{aa} & v^{ab} \\ v^{ab} & v^{bb} \end{bmatrix}, \quad \mathbb{T}(E) = \begin{bmatrix} t^{aa} & t^{ab} \\ t^{ab} & t^{bb} \end{bmatrix}. \quad (\text{A5})$$

Then the LSE becomes the algebraic equation,

$$\mathbb{T}(E) = \mathbb{V}(E) + \mathbb{V}(E) \mathbb{G}(E) \mathbb{T}(E), \quad (\text{A6})$$

with

$$\mathbb{G}(E) = \int \frac{d^3 \mathbf{q}}{(2\pi)^3} \mathbb{R}(\mathbf{q}) \mathcal{G}(\mathbf{q}, E) \mathbb{L}(\mathbf{q}), \quad (\text{A7})$$

$$\mathcal{G}(\mathbf{q}, E) = \frac{1}{E - m_a - m_b - \frac{\mathbf{q}^2}{2\mu} + i\epsilon}. \quad (\text{A8})$$

The formalism can be extended to a coupled-channel problem with the interaction

$$V_{ij}(\mathbf{p}', \mathbf{p}) = \mathbb{L}_i(\mathbf{p}') \mathbb{V}_{ij} \mathbb{R}_j(\mathbf{p}), \quad (\text{A9})$$

where i and j are the indices to label the channels. The interaction for a two-channel problem can be expressed explicitly,

$$V(\mathbf{p}', \mathbf{p}) = \mathbb{L}(\mathbf{p}') \mathbb{V} \mathbb{R}(\mathbf{p}) \quad (\text{A10}) \\ = \begin{bmatrix} \mathbb{L}_1(\mathbf{p}') \\ \mathbb{L}_2(\mathbf{p}') \end{bmatrix} \begin{bmatrix} \mathbb{V}_{11} & \mathbb{V}_{12} \\ \mathbb{V}_{12} & \mathbb{V}_{22} \end{bmatrix} \begin{bmatrix} \mathbb{R}_1(\mathbf{p}) \\ \mathbb{R}_2(\mathbf{p}) \end{bmatrix}.$$

With the factorization $T(\mathbf{p}', \mathbf{p}) = \mathbb{L}(\mathbf{p}') \mathbb{T} \mathbb{R}(\mathbf{p})$, the LSEs becomes algebraic equations

$$\mathbb{T}(E) = \mathbb{V}(E) + \mathbb{V}(E) \mathbb{G}(E) \mathbb{T}(E), \quad (\text{A11})$$

where

$$\mathbb{G} = \int \frac{d^3 \mathbf{q}}{(2\pi)^3} \begin{bmatrix} \mathbb{R}_1(\mathbf{q}) \mathcal{G}_1 \mathbb{L}_1(\mathbf{q}) & \\ & \mathbb{R}_2(\mathbf{q}) \mathcal{G}_2 \mathbb{L}_2(\mathbf{q}) \end{bmatrix} \quad (\text{A12})$$

where \mathcal{G}_i is the corresponding propagator in the i th channel.

ACKNOWLEDGMENTS

We are grateful to the helpful discussions with Prof. Oka Makoto and Xin-Zhen Weng. This project was supported by the National Natural Science Foundation of China (11975033 and 12070131001). This project was also funded by the Deutsche Forschungsgemeinschaft (DFG, German Research Foundation, Project ID 196253076-TRR 110). G.J. Wang was supported by JSPS KAKENHI (No.20F20026).

- [1] R. Aaij *et al.* (LHCb), (2020), [arXiv:2012.10380 \[hep-ex\]](#).
- [2] M. Ablikim *et al.* (BESIII), *Phys. Rev. Lett.* **126**, 102001 (2021).
- [3] R. Aaij *et al.* (LHCb), (2021).
- [4] H.-X. Chen, W. Chen, X. Liu, and S.-L. Zhu, *Phys. Rept.* **639**, 1 (2016).
- [5] F.-K. Guo, C. Hanhart, U.-G. Meißner, Q. Wang, Q. Zhao, and B.-S. Zou, *Rev. Mod. Phys.* **90**, 015004 (2018).
- [6] Y.-R. Liu, H.-X. Chen, W. Chen, X. Liu, and S.-L. Zhu, *Prog. Part. Nucl. Phys.* **107**, 237 (2019).
- [7] S. L. Olsen, T. Skwarnicki, and D. Zieminska, *Rev. Mod. Phys.* **90**, 015003 (2018).
- [8] N. Brambilla, S. Eidelman, C. Hanhart, A. Nefediev, C.-P. Shen, C. E. Thomas, A. Vairo, and C.-Z. Yuan, *Phys. Rept.* **873**, 1 (2020).
- [9] A. Esposito, A. Pilloni, and A. D. Polosa, *Phys. Rept.* **668**, 1 (2017).
- [10] B. Wang, L. Meng, and S.-L. Zhu, *Phys. Rev. D* **101**, 034018 (2020).
- [11] R. Aaij *et al.* (LHCb), *Phys. Rev. Lett.* **115**, 072001 (2015).
- [12] R. Aaij *et al.* (LHCb), *Phys. Rev. Lett.* **122**, 222001 (2019).
- [13] J. Ferretti and E. Santopinto, *JHEP* **04**, 119 (2020).
- [14] L. Meng, B. Wang, and S.-L. Zhu, *Phys. Rev. D* **102**, 111502 (2020).
- [15] Z. Yang, X. Cao, F.-K. Guo, J. Nieves, and M. P. Valderrama, (2020), [arXiv:2011.08725 \[hep-ph\]](#).
- [16] X. Cao, J.-P. Dai, and Z. Yang, *Eur. Phys. J. C* **81**, 184 (2021).
- [17] M.-C. Du, Q. Wang, and Q. Zhao, (2020), [arXiv:2011.09225 \[hep-ph\]](#).
- [18] B. Wang, L. Meng, and S.-L. Zhu, *Phys. Rev. D* **103**, L021501 (2021).
- [19] Q.-N. Wang, W. Chen, and H.-X. Chen, (2020), [arXiv:2011.10495 \[hep-ph\]](#).
- [20] Z.-F. Sun and C.-W. Xiao, (2020), [arXiv:2011.09404 \[hep-ph\]](#).
- [21] R. Chen and Q. Huang, *Phys. Rev. D* **103**, 034008 (2021).
- [22] J.-Z. Wang, Q.-S. Zhou, X. Liu, and T. Matsuki, *Eur. Phys. J. C* **81**, 51 (2021).
- [23] K. Azizi and N. Er, *Eur. Phys. J. C* **81**, 61 (2021).
- [24] X. Jin, X. Liu, Y. Xue, H. Huang, and J. Ping, (2020), [arXiv:2011.12230 \[hep-ph\]](#).
- [25] B.-D. Wan and C.-F. Qiao, (2020), [arXiv:2011.08747 \[hep-ph\]](#).
- [26] M.-Z. Liu, Y.-W. Pan, and L.-S. Geng, *Phys. Rev. D* **103**, 034003 (2021).
- [27] R. Chen, *Phys. Rev. D* **103**, 054007 (2021).
- [28] F.-Z. Peng, M.-J. Yan, M. Sánchez Sánchez, and M. P. Valderrama, (2020), [arXiv:2011.01915 \[hep-ph\]](#).
- [29] H.-X. Chen, W. Chen, X. Liu, and X.-H. Liu, (2020), [arXiv:2011.01079 \[hep-ph\]](#).
- [30] C.-W. Shen, H.-J. Jing, F.-K. Guo, and J.-J. Wu, *Symmetry* **12**, 1611 (2020).
- [31] F. Stancu, *Phys. Rev. D* **101**, 094007 (2020).
- [32] N. Ikeno, R. Molina, and E. Oset, *Phys. Lett. B* **814**, 136120 (2021).
- [33] M.-J. Yan, F.-Z. Peng, M. Sánchez Sánchez, and M. Pavon Valderrama, (2021), [arXiv:2102.13058 \[hep-ph\]](#).
- [34] U. Özdem and K. Azizi, (2021), [arXiv:2102.09231 \[hep-ph\]](#).
- [35] R. M. Albuquerque, S. Narison, and D. Rabetiarivony, (2021), [arXiv:2101.07281 \[hep-ph\]](#).
- [36] Y.-J. Xu, Y.-L. Liu, C.-Y. Cui, and M.-Q. Huang, (2020), [arXiv:2011.14313 \[hep-ph\]](#).
- [37] N. Ikeno, R. Molina, and E. Oset, *Phys. Lett. B* **814**, 136120 (2021).
- [38] Y. A. Simonov, (2020), [arXiv:2011.12326 \[hep-ph\]](#).
- [39] Z.-G. Wang, (2020), [arXiv:2011.10959 \[hep-ph\]](#).
- [40] J.-Z. Wang, D.-Y. Chen, X. Liu, and T. Matsuki, (2020), [arXiv:2011.08501 \[hep-ph\]](#).
- [41] M.-Z. Liu, J.-X. Lu, T.-W. Wu, J.-J. Xie, and L.-S. Geng, (2020), [arXiv:2011.08720 \[hep-ph\]](#).
- [42] Z. Q. Liu *et al.* (Belle), *Phys. Rev. Lett.* **110**, 252002 (2013), [Erratum: *Phys.Rev.Lett.* 111, 019901 (2013)].
- [43] M. Ablikim *et al.* (BESIII), *Phys. Rev. Lett.* **110**, 252001 (2013).
- [44] M. Ablikim *et al.* (BESIII), *Phys. Rev. Lett.* **111**, 242001 (2013).
- [45] H.-X. Chen, (2021), [arXiv:2103.08586 \[hep-ph\]](#).
- [46] L. Maiani, A. D. Polosa, and V. Riquer, (2021), [arXiv:2103.08331 \[hep-ph\]](#).
- [47] X. Liu, H. Huang, J. Ping, t. D. Chen, and X. Zhu, (2021), [arXiv:2103.12425 \[hep-ph\]](#).
- [48] P. G. Ortega, D. R. Entem, and F. Fernández, (2021), [arXiv:2103.07871 \[hep-ph\]](#).
- [49] X. Chen, Y. Tan, and Y. Chen, (2021), [arXiv:2103.07347 \[hep-ph\]](#).
- [50] Y.-H. Ge, X.-H. Liu, and H.-W. Ke, (2021), [arXiv:2103.05282 \[hep-ph\]](#).
- [51] M. Ablikim *et al.* (BESIII), *Phys. Rev. D* **92**, 092006 (2015).
- [52] M. Ablikim *et al.* (BESIII), *Phys. Rev. Lett.* **112**, 132001 (2014).
- [53] L. Meng, B. Wang, and S.-L. Zhu, (2020), [arXiv:2012.09813 \[hep-ph\]](#).
- [54] L. Meng, B. Wang, G.-J. Wang, and S.-L. Zhu, *Phys. Rev. D* **100**, 014031 (2019).
- [55] B. Wang, L. Meng, and S.-L. Zhu, *JHEP* **11**, 108 (2019).
- [56] M. Albaladejo, F.-K. Guo, C. Hidalgo-Duque, and J. Nieves, *Phys. Lett. B* **755**, 337 (2016).
- [57] R. Machleidt, *Computational nuclear physics. Vol. 2: Nuclear reactions*, edited by K. Langanke, S. E. Koonin, and J. A. Maruhn (Springer-Verlag, 1993) Chap. 1, pp. 1–29.
- [58] E. Epelbaum, J. Gegelia, and U.-G. Meißner, *Nucl. Phys. B* **925**, 161 (2017).
- [59] Z.-H. Guo and J. A. Oller, *Phys. Rev. D* **103**, 054021 (2021).
- [60] P. A. Zyla *et al.* (Particle Data Group), *PTEP* **2020**, 083C01 (2020).
- [61] L. Ma, W.-Z. Deng, X.-L. Chen, and S.-L. Zhu, (2015), [arXiv:1512.01938 \[hep-ph\]](#).
- [62] G.-J. Wang, L. Ma, X. Liu, and S.-L. Zhu, *Phys. Rev. D* **93**, 034031 (2016).